

Supporting information

Fabrication of AgCu/TiO₂ Nanoparticles Based Sensor for Selective Detection of Xylene Vapor

Popoti J. Maake^{1,2}, Teboho P. Mokoena³, Amogelang S. Bolokang⁴, Nomso Hintsho-Mbita⁵, James Tshilongo⁶ Franscious R. Cummings⁶ Hendrik C. Swart³, Emmanuel I. Iwuoha², David E. Motaung^{3*}

¹DST/CSIR National Centre for Nanostructured Materials, Council for Scientific Industrial Research, Pretoria 0001, South Africa

²Sensor Lab, Chemistry Department, University of the Western Cape, Private Bag X17, Bellville 7535, South Africa

³Department of Physics, University of the Free State, P.O. Box 339, Bloemfontein ZA9300, South Africa

⁴Council for Scientific Industrial Research, Materials Science and Manufacturing, Advanced Materials and Engineering, Meiring Naude Road, P O Box 395, Pretoria, South Africa

⁵Department of Chemistry, University of Limpopo, Private Bag X1106, Sovenga, 0727, South Africa

⁶Mintek, Analytical Service Division, 200 Malibongwe Drive, Randburg 2194, South Africa

⁷Electron Microscopy Unit, University of the Western Cape, Bellville, 7535, South Africa

*Corresponding Author: David Motaung, Email: MotaungDE@ufs.ac.za

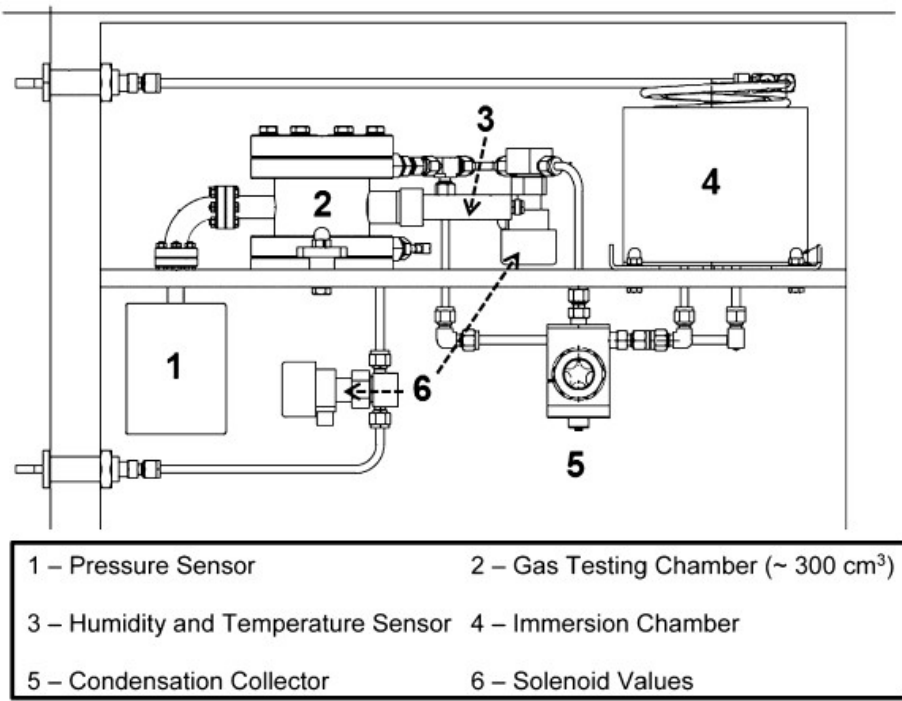


Fig. S1: Schematic diagram of the gas testing station used during the gas-sensing analyses.

Table S1. Summary of the crystallite size of AgCu/TiO₂

Materials	Lattice strain, ε ($\times 10^{-4}$)	Crystallite size (nm), L
Pure TiO ₂	0.0002	16.1
0.1% mol AgCu/TiO ₂	0.0005	13.1
0.5% mol. AgCu/TiO ₂	0.0004	17.2
0.5% mol Ag 0.1% mol Cu/TiO ₂	0.0009	8.5
0.1% mol Ag 0.5% mol Cu/TiO ₂	0.0053	9.8

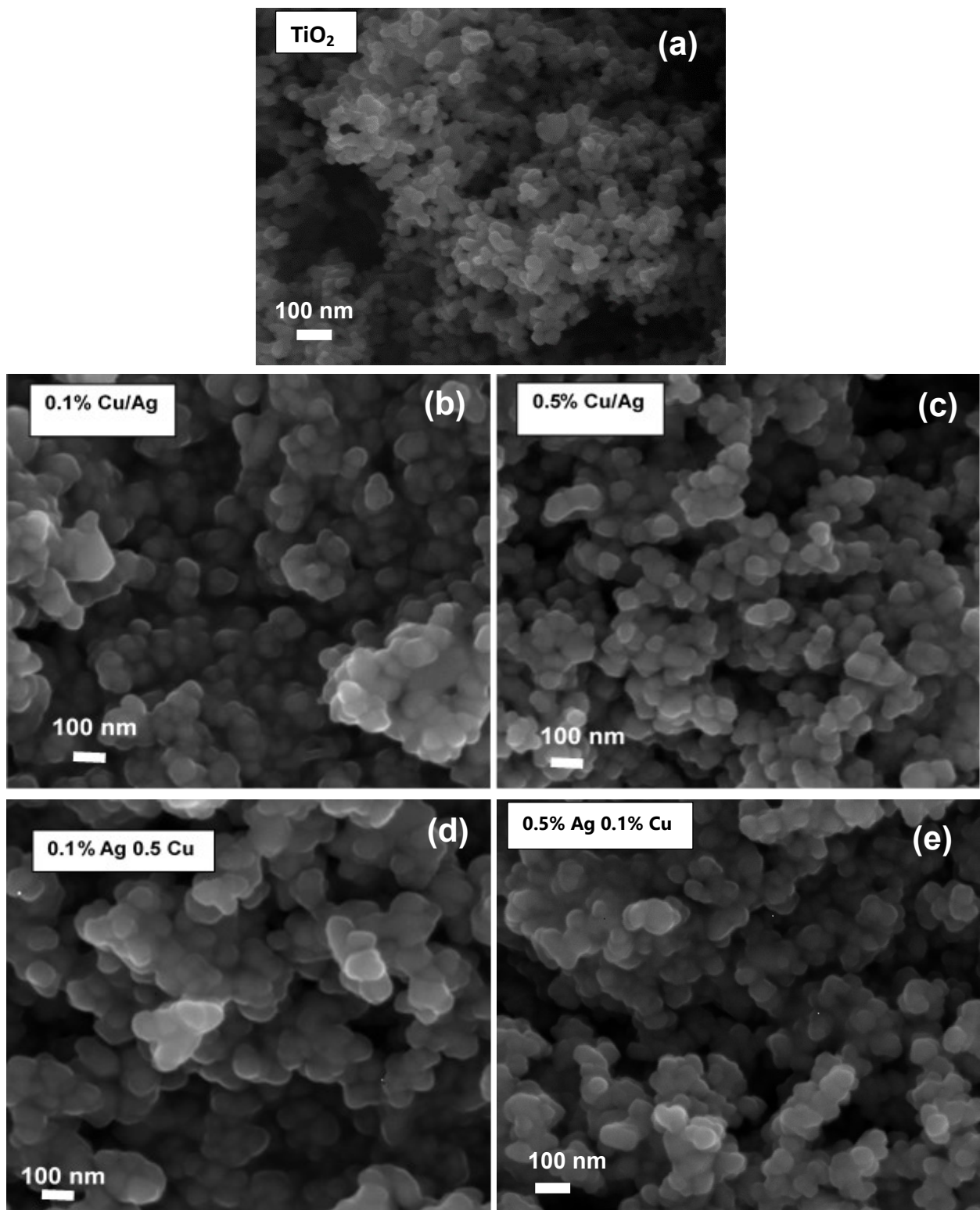


Fig. S2: EDX spectra of 0.1 mol.% AgCu/ TiO_2 nanostructured material.

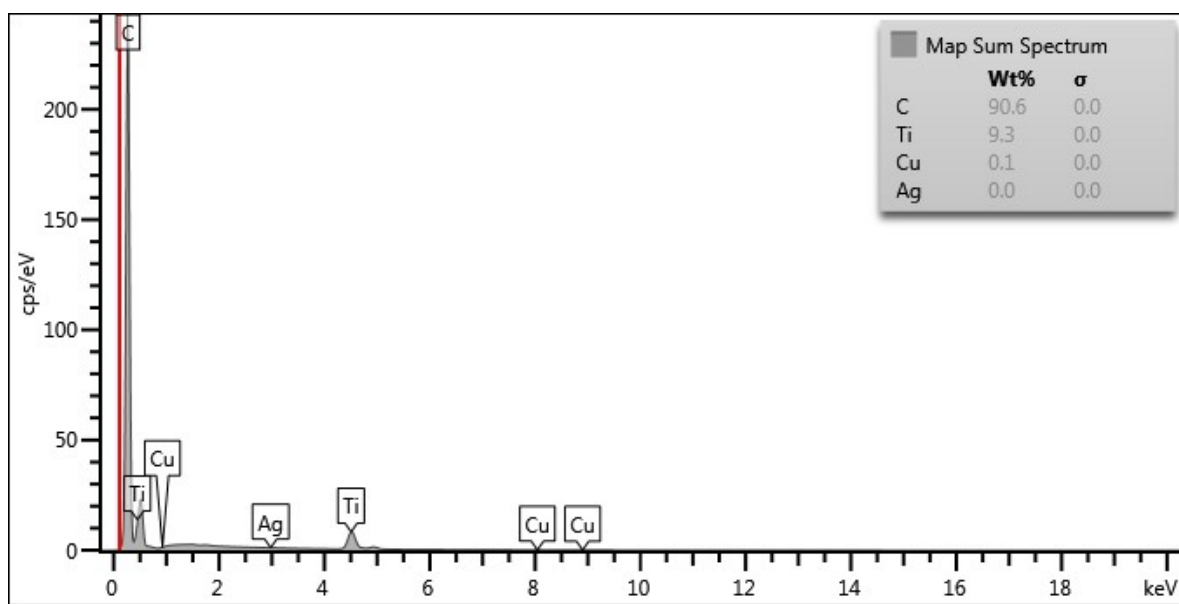


Fig. S3: EDX spectra of 0.5 mol.% AgCu/TiO₂ nanostructured material.

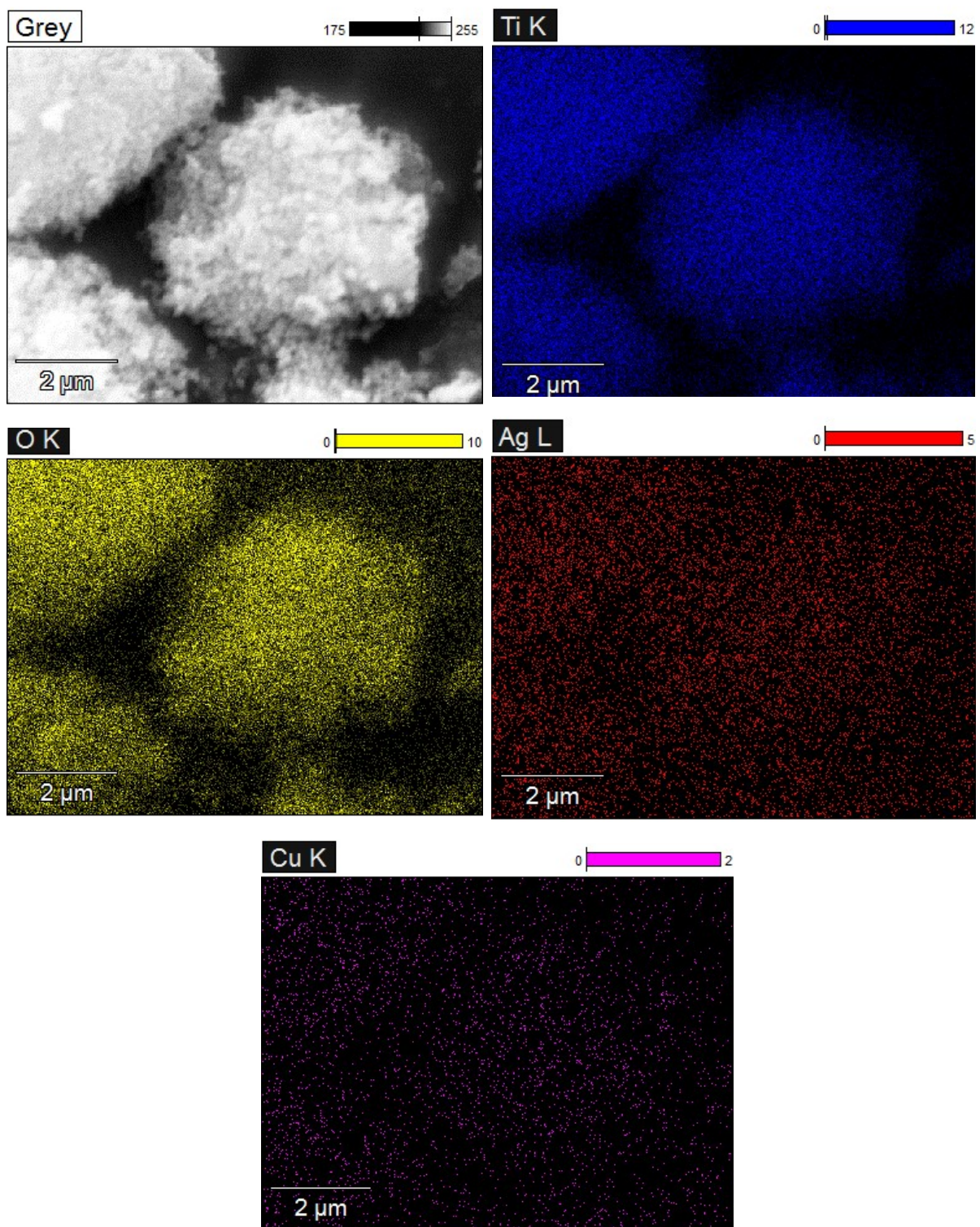


Fig. S4: EDS elemental mapping of 0.5 mol.% AgCu/TiO₂ nanoparticles.

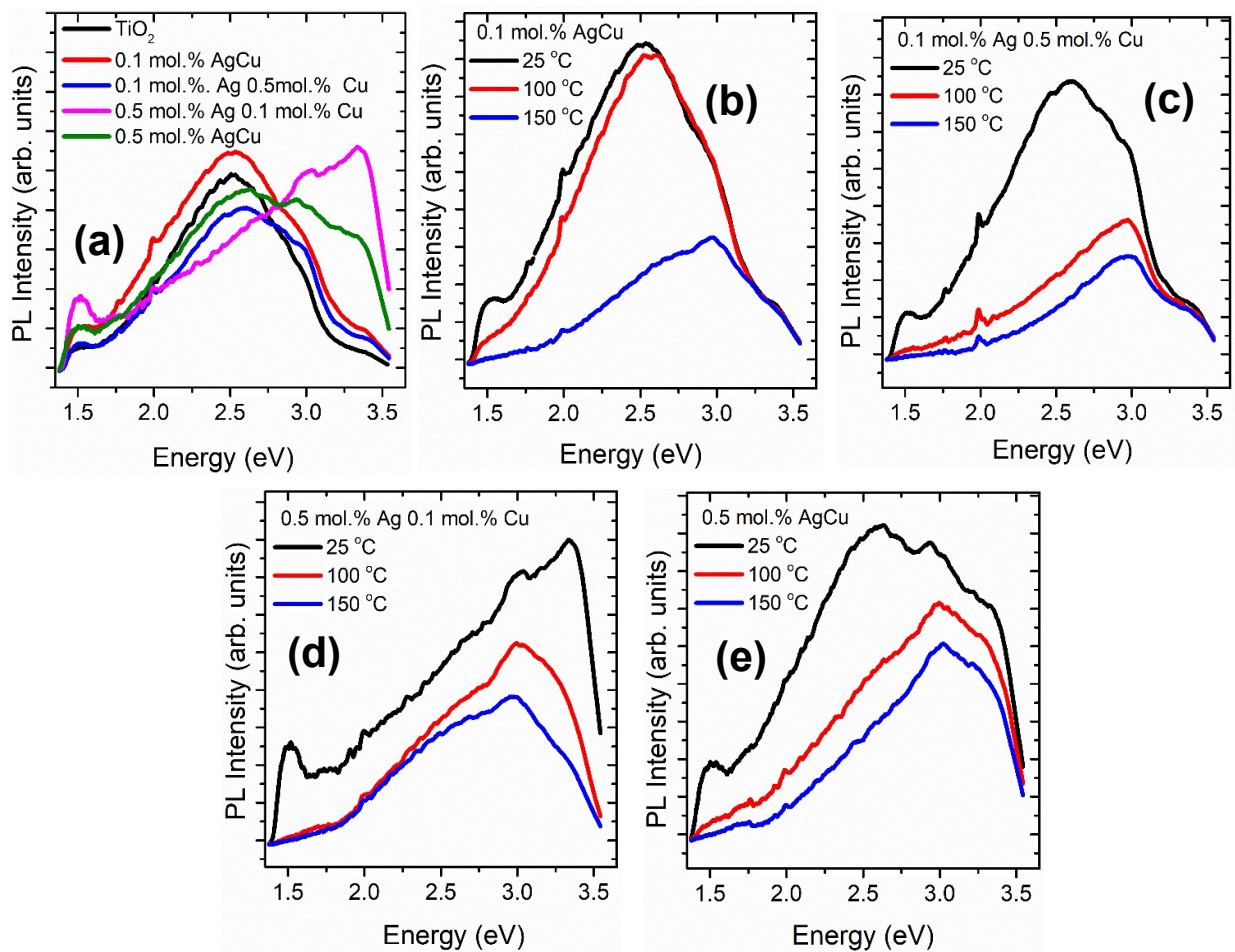


Fig. S5: Room temperature PL spectra of (a) undoped and AgCu/TiO₂ nanoparticles, and (b-e) In-situ PL spectra of AgCu/TiO₂ nanoparticles conducted from 25 to 150 °C.

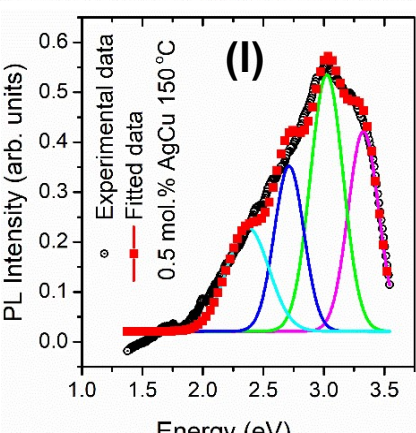
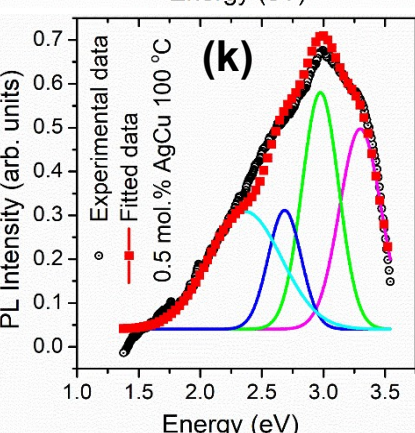
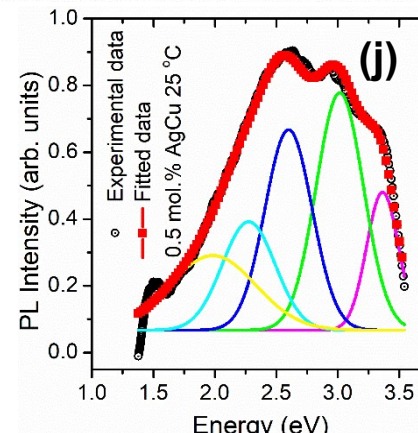
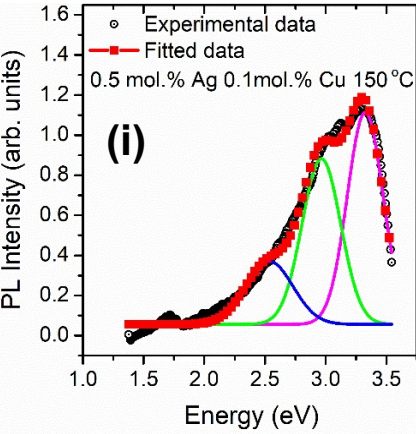
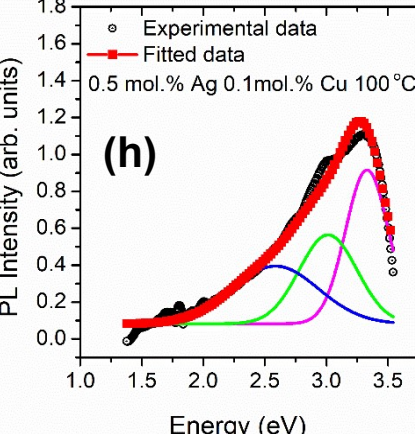
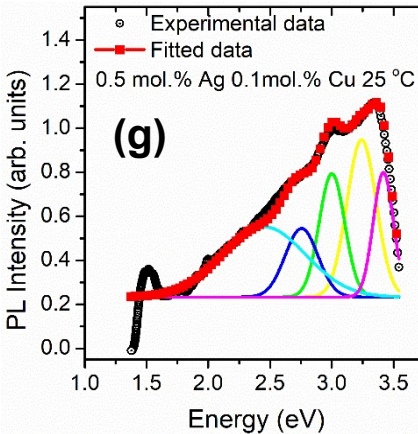
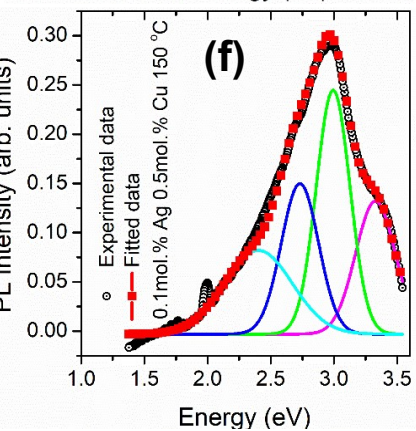
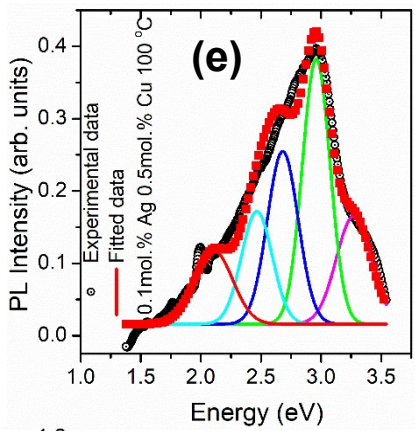
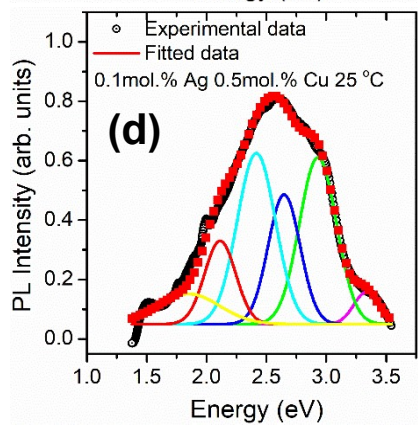
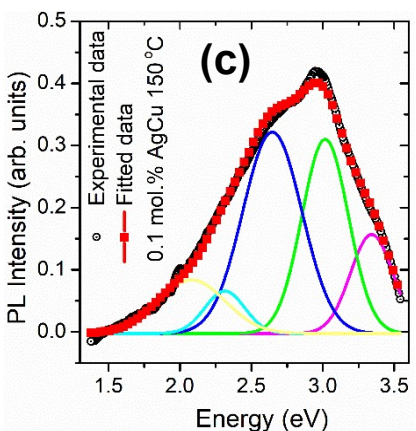
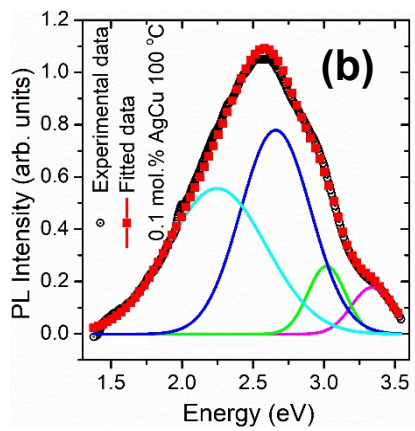
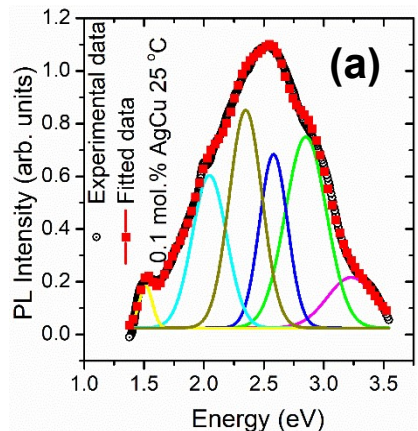


Fig. S6: In-situ PL fitted spectra of at different temperatures (a-c) 0.1 % mol. AgCu/TiO₂, (d-f) 0.1% mol. Ag 0.5 mol.% Cu/TiO₂, (g-i) 0.5% Ag 0.1% mol. Cu/TiO₂, (j-l) 0.5 % mol. Ag Cu/TiO₂ of at 25, 100 and 150 °C, respectively.

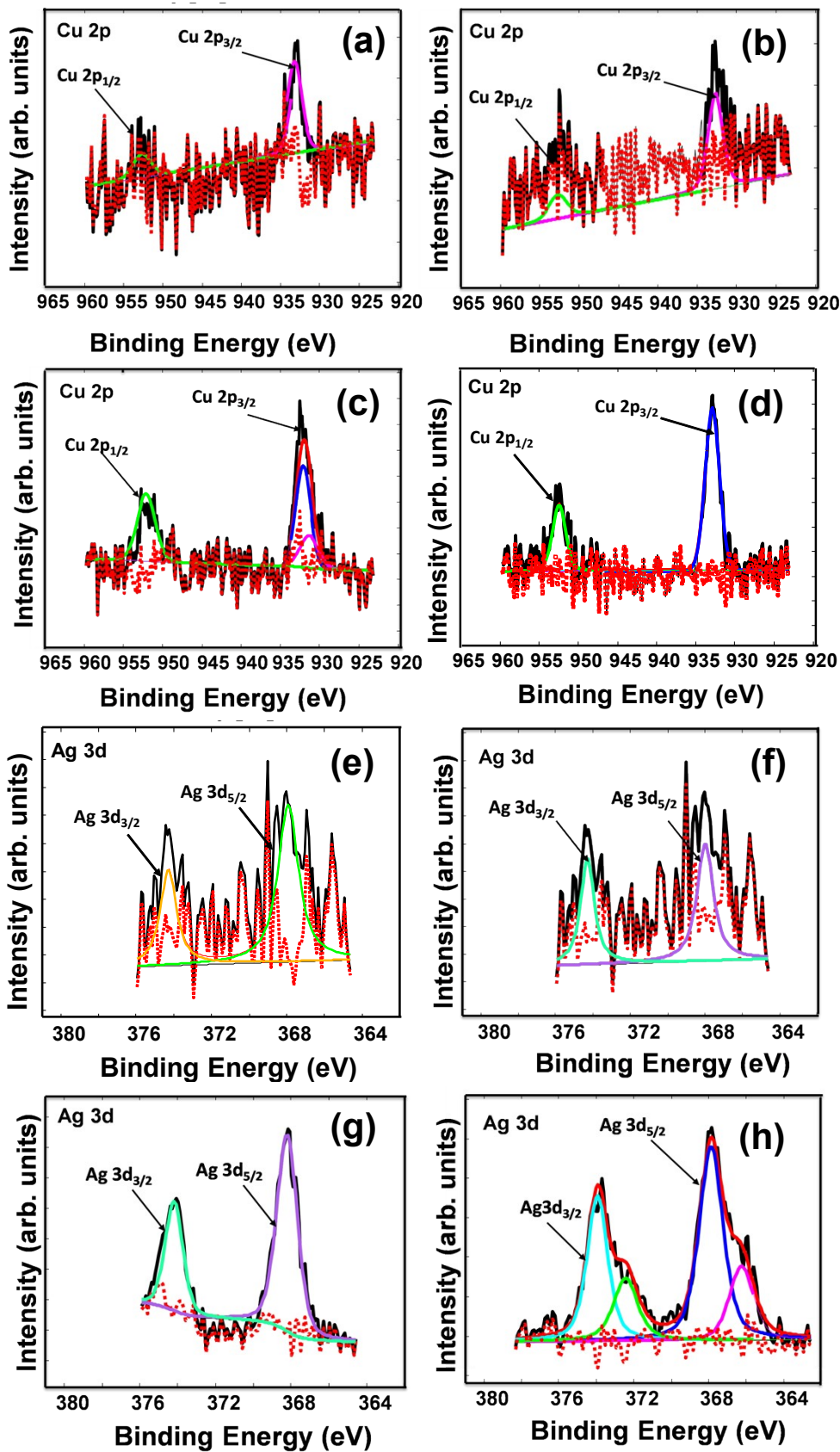


Fig. S7: (a-d) Cu2p of (a) 0.1 % mol. Ag Cu/TiO₂, (b) 0.1% mol. Ag 0.5 mol.%Cu/TiO₂, (c) 0.5 mol.% Ag 0.1 mol.% Cu/TiO₂, (d) 0.5 mol.% AgCu/TiO₂, (e-h) Ag 3d of (e) 0.1 % mol. Ag Cu/TiO₂, (f) 0.1% mol. Ag/0.5 mol.%Cu/TiO₂, (g) 0.5% Ag 0.1 mol.% Cu/TiO₂ (h) 0.5 mol.% AgCu/TiO₂ nanoparticles.

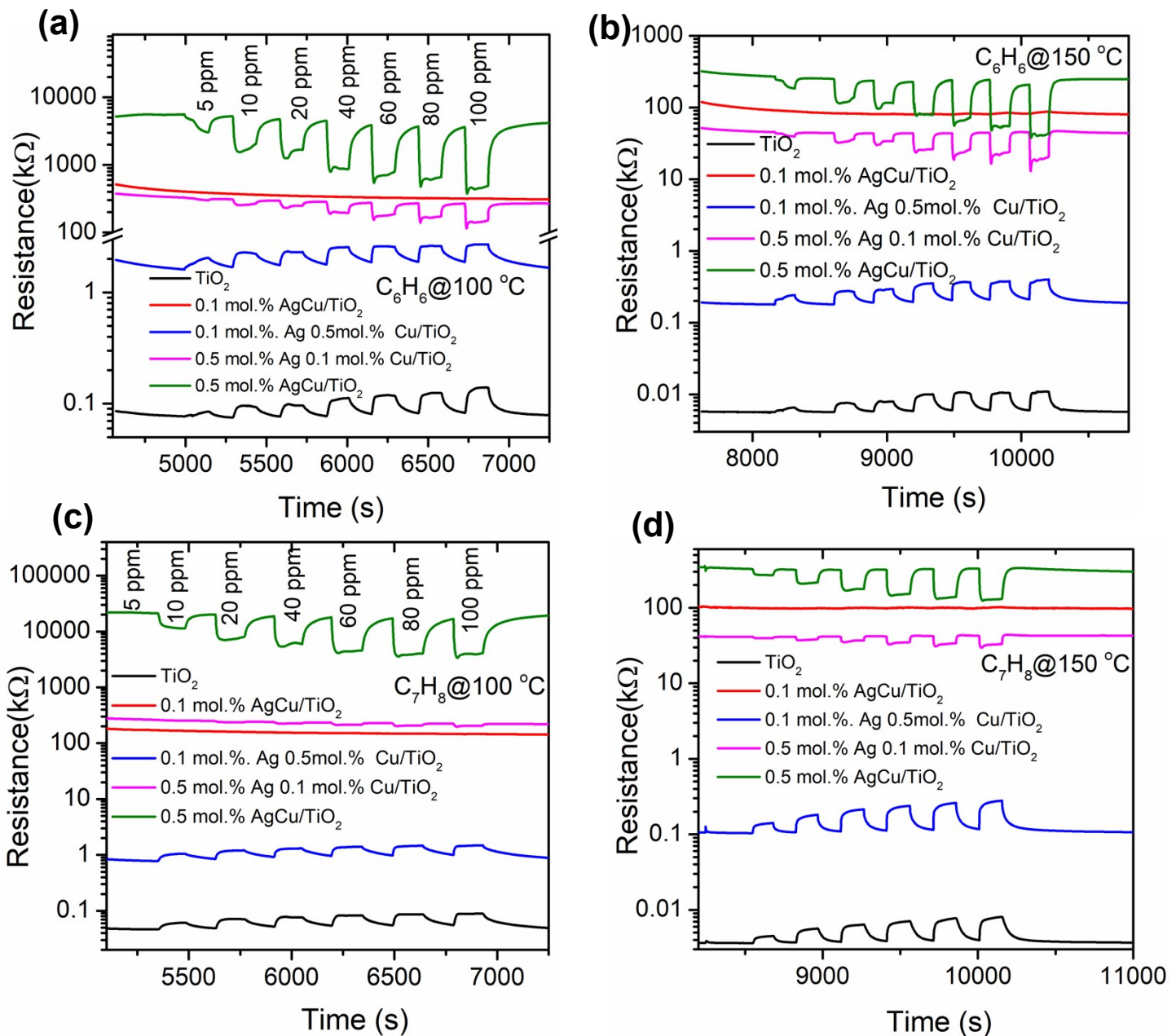


Fig. S8: Real-time resistance plot of various sensors tested to (a-b) benzene and (c and d) toluene vapours at 100 and 150 °C, respectively.

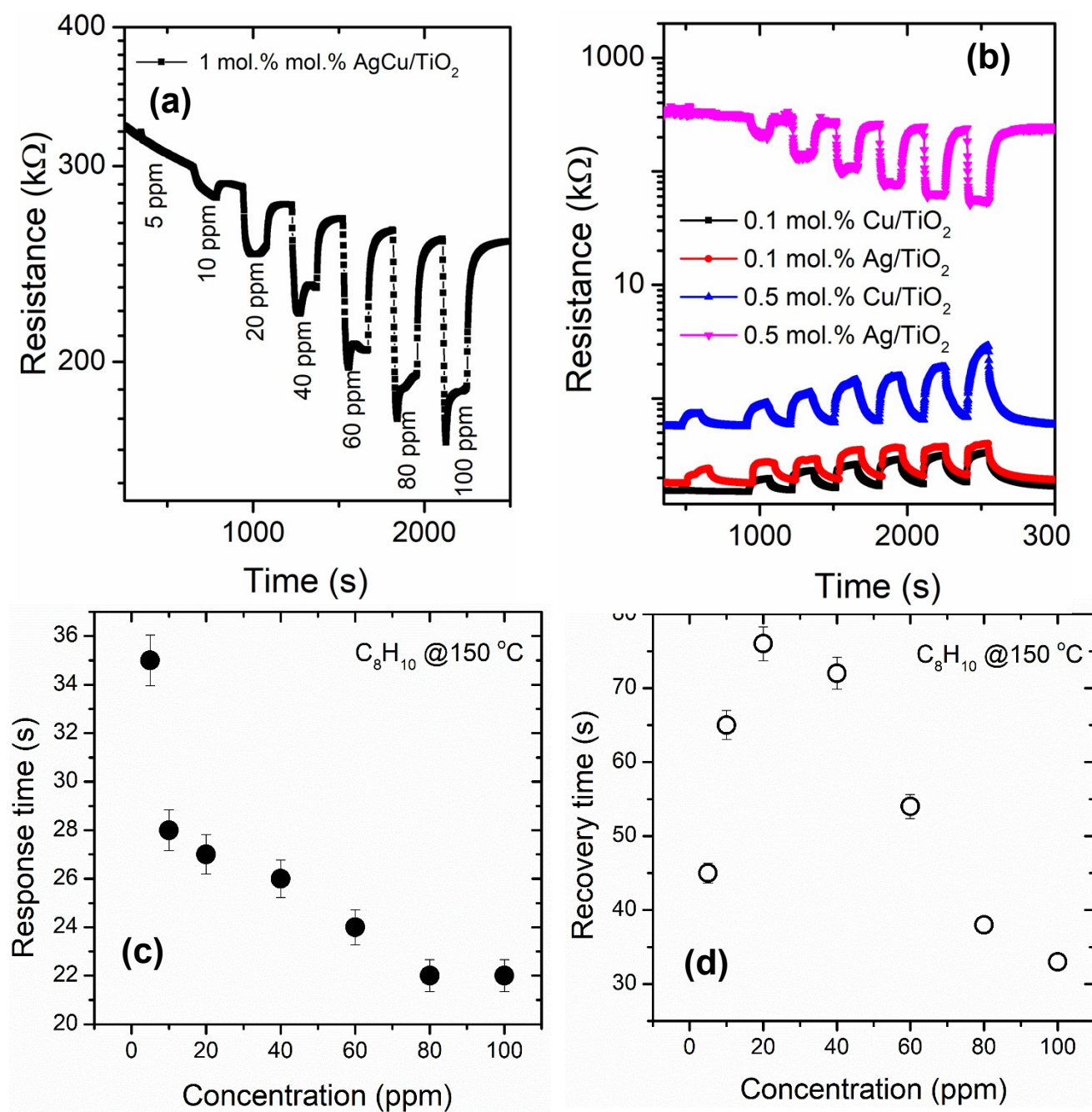


Fig. S9: (a) real-time response of various sensors towards xylene at 150 °C, (b) response time and (c) recovery time of 0.5 mol. % AgCu/TiO₂ based sensor towards xylene at 150 °C.

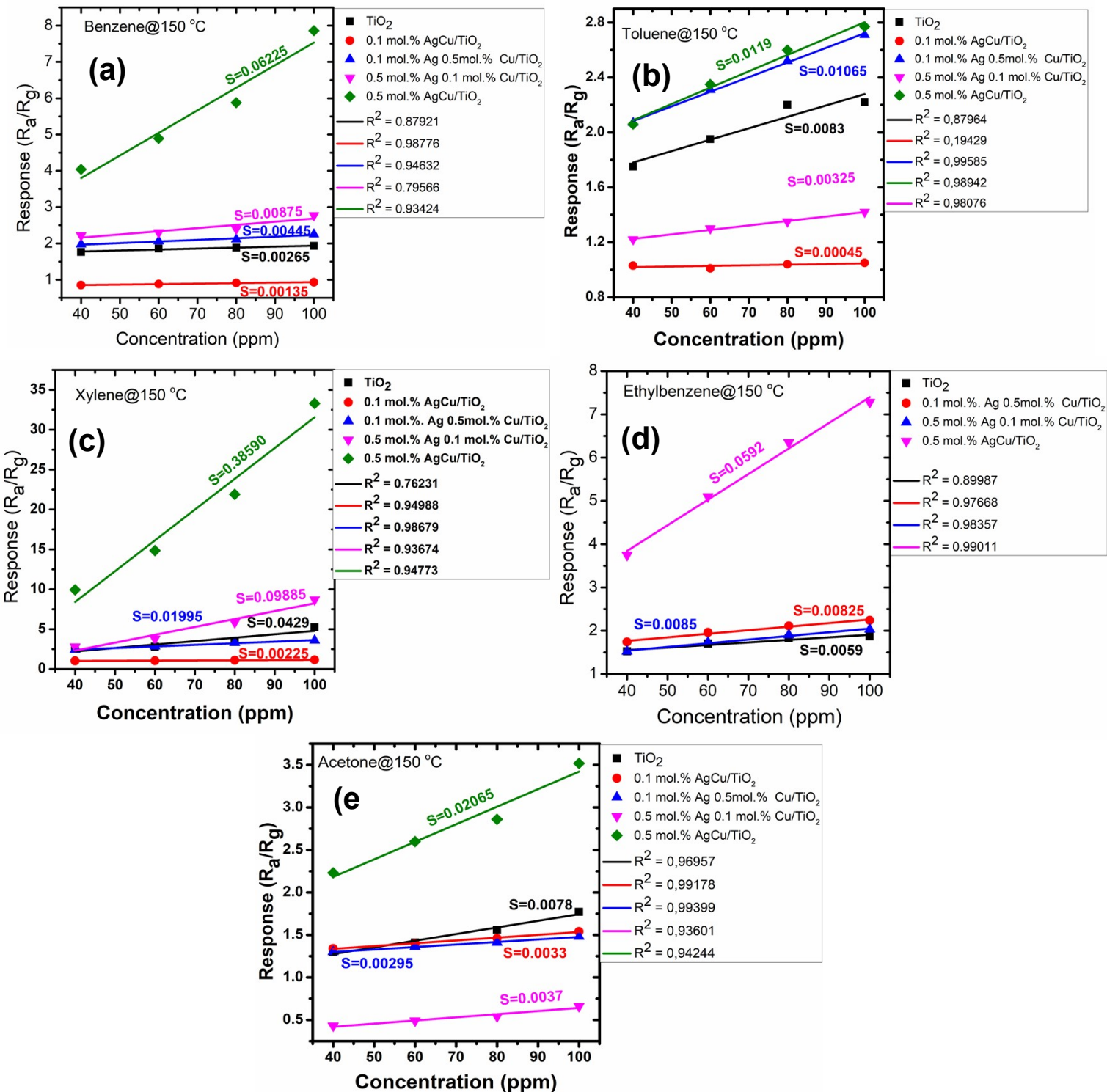


Fig. S10: Sensitivity of the various sensors measured towards different gases (a) benzene, (b) toluene, (c) xylene, (d) ethylbenzene and (e) acetone at 150 °C.

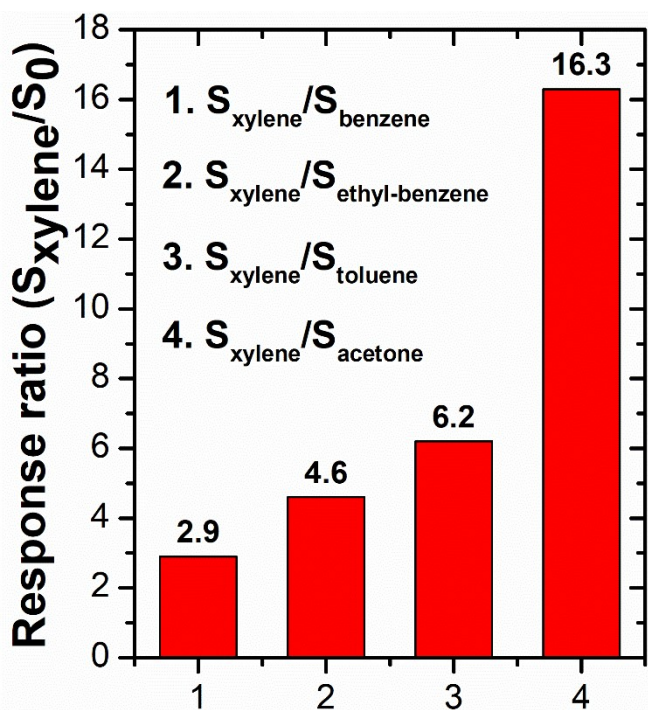
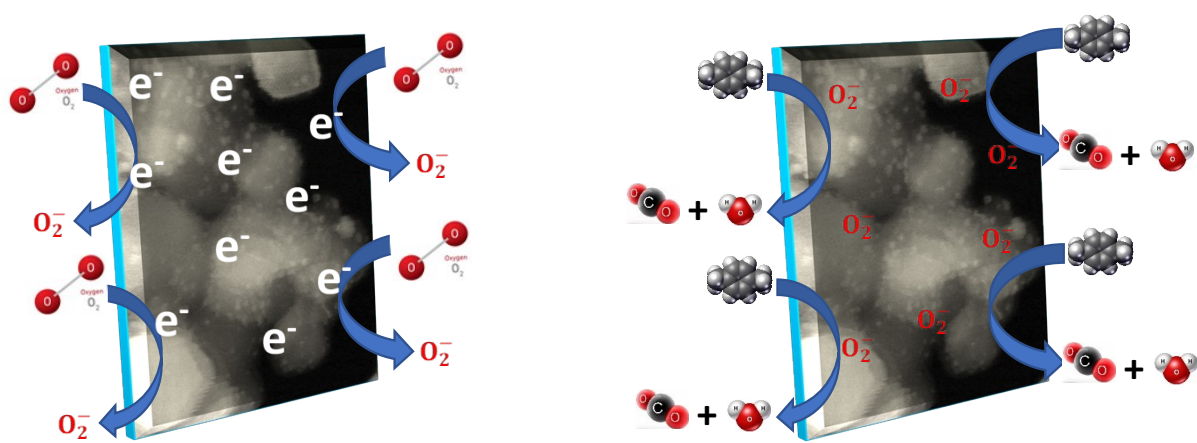


Fig. S11: Cross-sensitivity plot of 0.5 mol. % AgCu/TiO₂ based sensor towards other interference gases.

Materials	529 eV %	530 eV %	531 eV %	532 eV %
Pure TiO ₂		65.5	11.1	23.4
0.1 mol.% AgCu/TiO ₂	64.0	28.9	7.1	
0.1 mol.% Ag 0.5 mol.% Cu/TiO ₂	68.0	27.7	4.3	
0.5 mol.% Ag 0.1 mol.% Cu/TiO ₂	83.2	12.0	4.8	
0.5 mol.% AgCu/TiO ₂	20.0	63.9	16.1	

Table S2: Summary of XPS analyses



Scheme 1: Schematic drawing showing the gas sensing mechanism of AgCu/TiO₂ towards xylene vapour